International Journal of Engineering and Advanced Technology (IJEAT)
ISSN: 2249-8958 (Online), Volume-4 Issue-4, April 2015

Thermal Model for Prediction of Deposition Dimension of a Deposited Nickel Superalloy

A. Soleymani

Abstract— Reduction of the final cost of products, complexities of the geometry of the products, as well as speed of the productions are some of the reasons for using rapid prototyping methods in material fabrication processes. Rapid prototyping enables the user to make near net-shape products. Having a good understanding of the thermal history is one of the main challenges of the materials made by rapid prototyping methods. Since the final product is gradually made under a continuous process, a small area can be heated multiple times during different passes of depositions. A series of heating and cooling (with different rates) cycles can importantly affects the microstructural evolution and the chemical compositions (in the case of alloys). In this paper, a finite-element-based thermal model for the manufacturing of nickel-based superalloy on a steel substrate heated by a laser source was developed using COMSOL multiphysics software. The model was assessed based on measuring and comparing the depth and width of the molten with the reported values in the literature. The model results were in good agreement (maximum error of 16%) with the experimental results available in the literature. It was concluded that the developed thermal model can be used for the optimization of the used parameters in the manufacturing process in order to get the desired properties.

Keywords—Thermal model, Finite elements, rapid prototyping, Nickel

I. INTRODUCTION

Producing materials with less depletion of the raw material, manufacturing complex-shape materials and fabricating more environmentally friendly materials are only few of the benefits of advanced manufacturing methods compared to conventional material processing methods such as casting. Rapid manufacturing can be considered as one of the most innovative methods of manufacturing that gains lots of attentions these days. In some rapid manufacturing methods, material is added gradually (either as powder or wire) and it is locally melted and added to the bulk material. Each part of the material experiences multiple heating and cooling cycles. These heating and cooling considerably affect the mechanical properties of the final product because of influencing the microstructural evolution as well as composition variation in different parts of the deposited sample. For instance, it is of great interest to know the optimum scan velocity for the minimum residual stress induced by the temperature field (i.e., gradient) in a steel sample made by a rapid manufacturing method. The most important factor controlling the properties of the manufactured materials is the variation of temperature along the sample during the deposition. The variation of temperature is mostly because of the local molten pool that is exploring most of the sample more than once.

Manuscript published on 30 April 2015.
***** Correspondence Author (s)
Amir Soleymani, Department of Mechanical and Manufacturing Engineering, University Putra Malaysia, Serdang, Malaysia.

In another word, a previously solidified region of the sample may experience a partial re-melting and solidification. This back and forth melting and cooling lead to the formation of a wide range of microstructure and composition changes in metallic alloys [1-4]. Thermal modeling has been done frequently to model rapid manufacturing methods. Finite element methods were used to model the deposition of a thin wall of stainless steel 316. In this study, the substrate temperature was assumed to be a fixed value. Also, conduction was considered as the only method of heat conduction. In another study, the role of parameters affecting the residual stress formed during the deposition because of the variation of the temperature and heat flux were investigated. In this study, the melt pool size and its geometry as a function of the laser velocity and the incident energy were investigated. The developed model considered conductive heat flow and a moving point heat source. It was also considered that the substrate melting temperature changes negligibly. Similarly, another thermal model was developed in which the thermal gradient was used to justify the residual stress forms during the deposition . The thermal deposition of tool steel iron (AISI 420) was studied by Costa et. al. [5] using ABAQUS software in order to study the effect of thermal cycle on the microstructural evolutions. The developed model was later improved by putting the actual values for the thermal conduction of the material [6]. The laser energy distribution during the deposition for a thermal model was studied by Neela et. al. [7]. In this study a multistep, time dependent heat transfer model was developed. The heat source energy was considered to be a non-uniform Gaussian distribution. The other used parameters in this study were the powder mass flow, scanning velocity, and powder usage efficiency). The effect of temperature on the performance and properties of powders were studied by Patil et. al. [8]. In this research, the thermal distortion during cooling was reduced which resulted in improving the properties of the final product.

In this study, a time-dependent thermal model which is able to predict the temperature with respect to time and location was developed. The thermal model development was done using COMSOL multiphysics software to establish the model and solve the finite element problem. The validity of the thermal model was assessed by comparing the width and depth of a deposited Nickel superalloy formed on an iron substrate [9] with the thermal model results. The effects of important parameters (such as the scan velocity of the heat source as well as the variation of the heat power) on the size of the molten pool and subsequently on the deposition volume were considered.

Published By:
Blue Eyes Intelligence Engineering and Sciences Publication (BEIESP)

II. THERMAL MODEL DEVELOPMENT

COMSOL multiphysics 4.4 was used to simulate the temperature variation of a metallic alloy deposited by a laser heat source. The role of COMSOL was to develop the thermal model, solve the finite element model and do post processing on the results. The most important task of the COMSOL software is to solve the partial differential equation selected for the developed finite element model. In this case, the COMSOL software tries to solve the partial differential equation by numerical methods using nods made during the mesh process. As soon as the partial differential equation is solved, the results are used for further post processing. The inputs of the thermal model were material properties such as heat capacity, density and thermal conductivity, heat source power, the speed of the heat source motion, time of the deposition, ambient temperature and pressure, thermal reflectivity coefficient, and sample dimensions. The flowchart of the study is shown in Fig. 1.

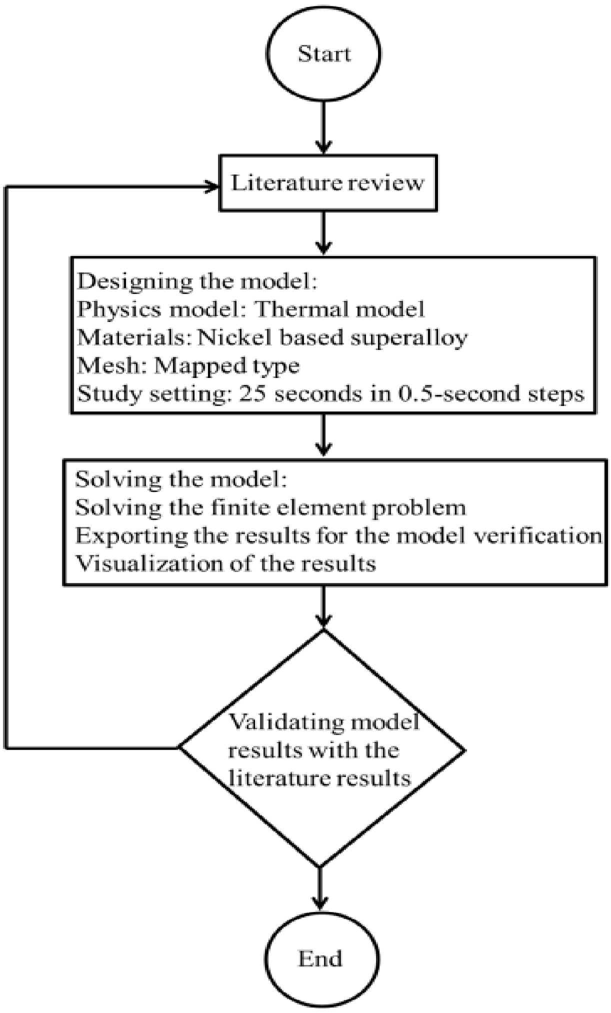

Fig. 1: Flowchart of the study

Primarily, the global parameters were set. Some of these parameters can be named as follow: preheat of the powder which is 300 K (i.e., there is no preheating of the powder), preheat of the substrate which is 300 K, etc. The parameters used to make the thermal model are presented in Table 1.

The second part of the global parameters is the ‘HeatInput’ function which controls the motion and the intensity (as well as its distribution) of the laser heat source. The inputs of this function are x, y, and t. The schematic of the power distribution in the heat source is shown in Fig. 2. In Fig. 2, it is shown that at the moment of 18.5 seconds, the heat source is in the middle of the way of deposition. The total power of the heat source was ~ 900 W.

Table 1 Parameters used to make the thermal model

Parameter	Value
Initial temperature	273 K
Power	900 W
Scan velocity	2 mm/s
Total time of deposition	25 s
Steel melting point	1813 K
Nickel superalloy melting point	1605 K

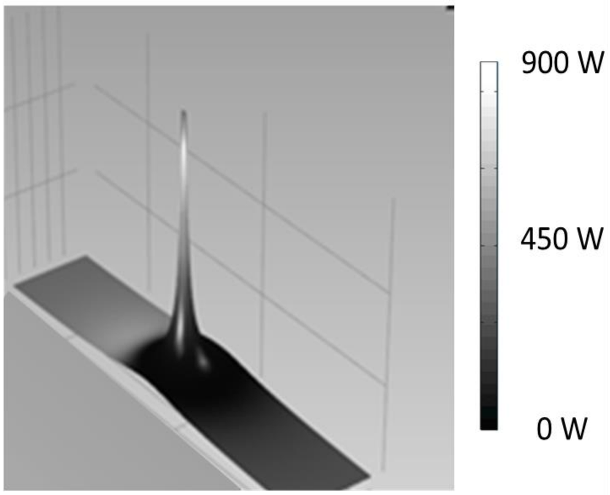

Fig. 2 Heat source schematic at an arbitrary angle

The function which was used to make the symmetric heat distribution in the x-y plane is called Gaussian pulse. This function is a common bell-shaped curve. This shape is similar to the normal Gaussian distribution. Similar to the normal distribution, it is possible to make Gaussian pulse according to Eq. (1)

$$y(r)=\frac{1}{\sigma\sqrt{2\pi}}e^{\frac{-(r-r_0)^2}{2\sigma^2}} \quad (1)$$

Where *r* represents the distance axis of the polar coordinate and it can be easily calculated by the square root of the summation of the squares of the *x* and *y* values. Also, □ is the standard deviation of the heat source from its optic axis which set as 0.002.

The geometry of the problem had two main parts. The first part was the substrate (the bottom part in Fig. (3-a)) and the second part was the going to be deposited sample (the top part in Fig. (3-a)). The width, length and height of the substrate are 0.06 m, 0.06 m and 0.01 m, respectively and the corner was located at the -0.025 m, -0.005 m and 0, respectively. The width, length an height of the deposited layer were 0.01 m, 0.05 m and 0.01 m, respectively and the corner was located at the 0 m, 0 m and 0.01, respectively. The axis type for both substrate and the deposition layer was set to z-axis and the rotation angle was zero.

Published By:
Blue Eyes Intelligence Engineering
and Sciences Publication (BEIESP)

Finally, the assembly was done to make the complete geometry union (Fig. (3-a)). The type of the applied mesh to the geometry was 'mapped out' as shown in Fig. (3-b).

The geometry of the problem contained two parts which were the substrate and the deposition layer. However, the number of materials used in the thermal model was three. The first material was related to the substrate. This material is steel A302 Grade B. The second material was related to the deposition layer which was Nickel superalloy powder. The material was related to the atmosphere around the substrate and the deposition layer. This atmosphere was argon gas. The material properties of all these three materials were provided by the metal's Handbook database. The key parameters for developing the thermal model are thermal conductivity, heat capacity at constant pressure and density. The used values for these parameters are shown in Fig. 4-6.

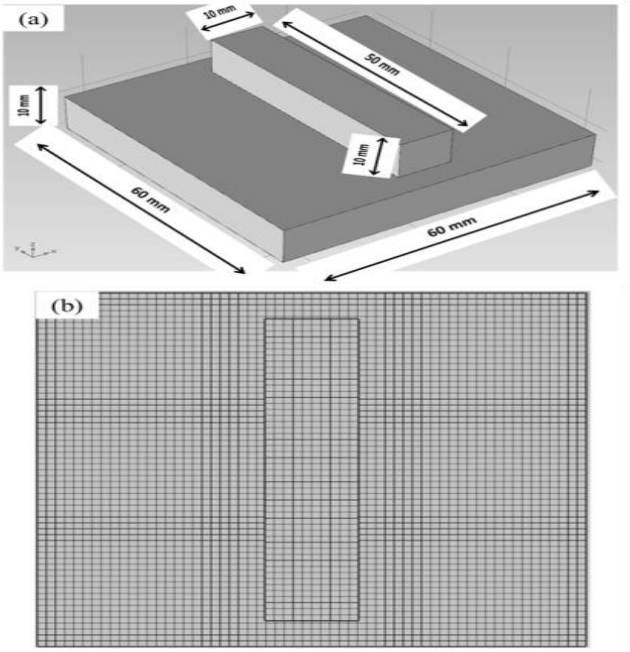

Fig. 3 Schematic of the substrate and the deposition

The equation that governs the heat transfer is shown in Eq. (2), where □ is the density, c_p is the heat capacity, T is the temperature, t is time, u is the velocity, and Q is the heat source input energy. The thermal model was solved based on the assumption that there was no variation in the pressure of the atmosphere (10^5 Pascal). Heat flux was applied only to the top surface surface shown in Fig. 3, according to Eq. (3) where q_{tot} is the total heat energy which was controlled by the 'HeatInput' function defined in the parameter part and A is the area over which the heat source is applied. The developed model was a time dependent model in which the temperature evolution with respect to time was solved. The time changed from 0 to 25 seconds. This problem was solved in 25 steps; i.e., with the resolution of 1 second. The solver configuration showed both time and temperature as the variables. This solver took the responsibility of the synchronization of the time and temperature during the time period of 25 seconds.

$$\rho c_p \frac{\partial T}{\partial t} + \rho c_p u.\nabla T = \nabla.(\nabla T) + Q$$

$$-\mathbf{n}.(-k\nabla T) = \frac{q_{tot}}{A}$$

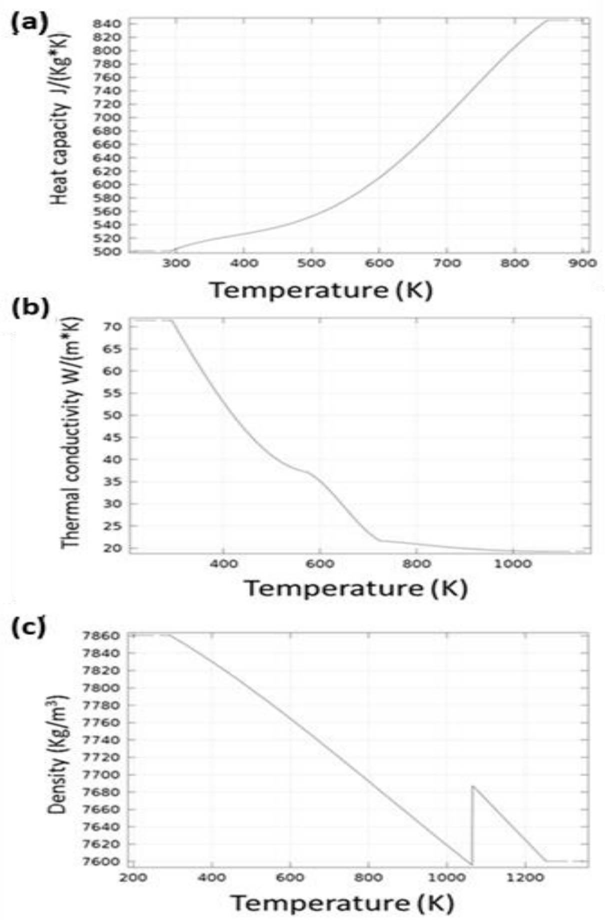

Fig. 4 Steel properties (a) heat capacity (b) thermal conductivity (c) density

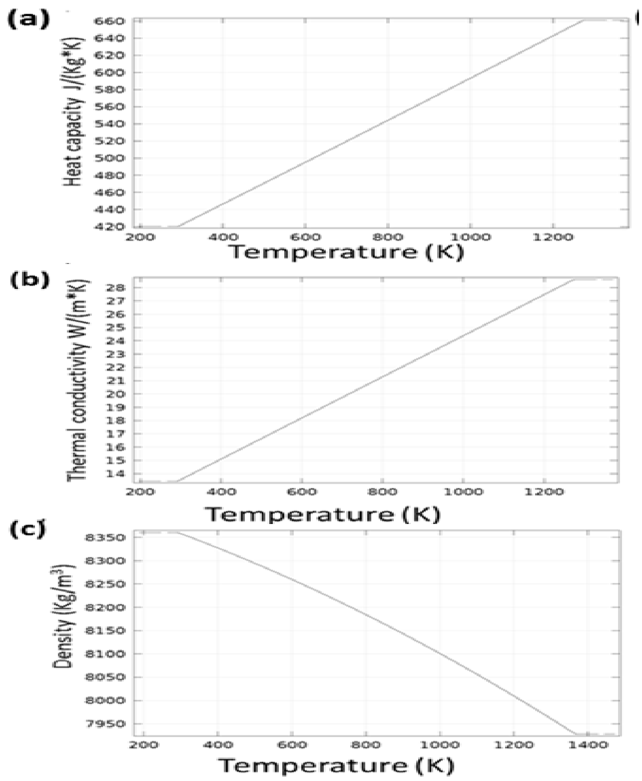

Fig. 5 Nickel properties (a) heat capacity (b) thermal conductivity (c) density)

Published By:
Blue Eyes Intelligence Engineering
and Sciences Publication (BEIESP)

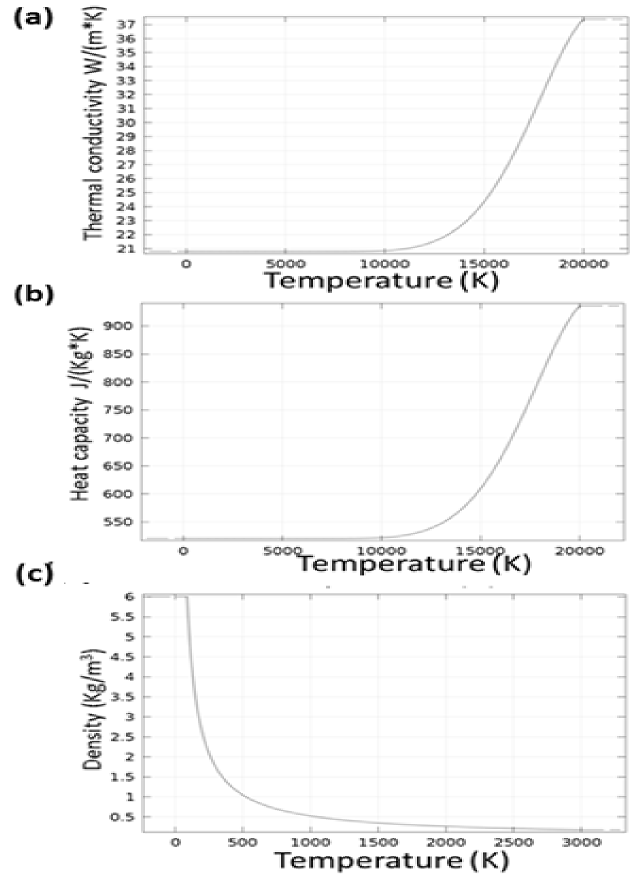

Fig. 6 Argon properties (a) thermal conductivity (b) heat capacity (c) density

III. RESULTS AND DISCUSSIONS

The schematic of the thermal model results provided by the COMSOL software are shown in Fig. 7 and Fig. 8. Fig. 7 presents the surface thermal model results at different time during the deposition. Particularly, since the heat source is laser, the heat concentration at a small area close to the laser source is a lot. This heat concentration increases the temperature of the local area in comparison to its adjacent area. Also at the beginning of the deposition, the substrate acts as a sink for heat because the initial temperature of the substrate is room temperature. Therefore the presence of the substrate increases the total time needed for the entire geometry to reach the steady state condition in the thermal model. Based on this delay, it is normally expected that the molten pool shape varies slightly. Also, the molten pool cannot be fully circular because of the anisotropy exists in the temperature field. To explain it more, it should be mentioned that the temperature field (or gradient) ahead of the heat source motion is far more in comparison to the back side (because the back side is already heated and its temperature is closer to the currently deposited area although the area ahead of the deposition is not heated yet. The role of the substrate is also essential in the formation of non-circular molten pool. As mentioned, at the initial moment of the deposition, the substrate is fully cold however, gradually it is heated and the temperature gradient forms in the substrate as well. This gradient intensifies the asymmetry exists in the molten pool. Also, it should be considered that the total time of the deposition is 25 seconds and the temperature range (difference between the highest and lowest temperatures) is ~2300 K. To extract the size of the molten pool iso-surface plots were used. The iso-surface plots were made at the molting temperature of the nickel superalloy (i.e. 1605 K). These plots are shown in Fig. 8. Because of the fact that the thermal model is far from the steady state condition, the shape of the molten pool slightly changes with respect to the elapsed time. To compare the results of this study with the literature, the average size of the molten pool in the first 25 seconds of the deposition (i.e., the total time of the deposition) is considered.

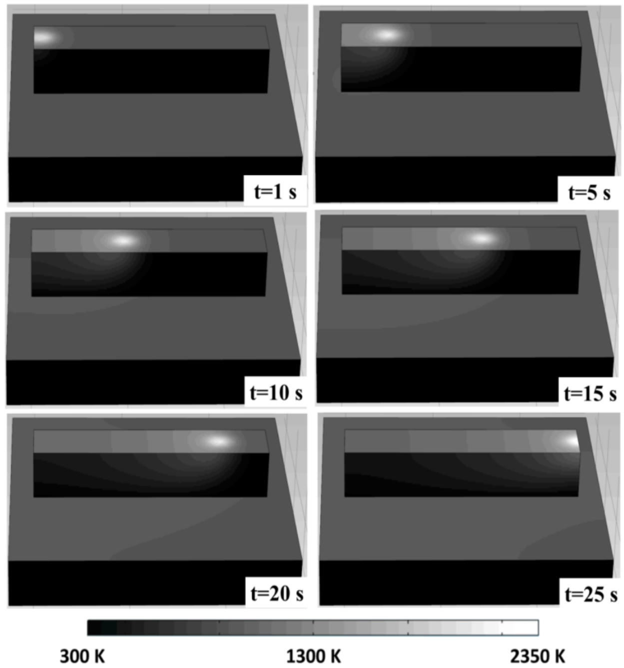

Fig. 7 The schematic of the thermal model results

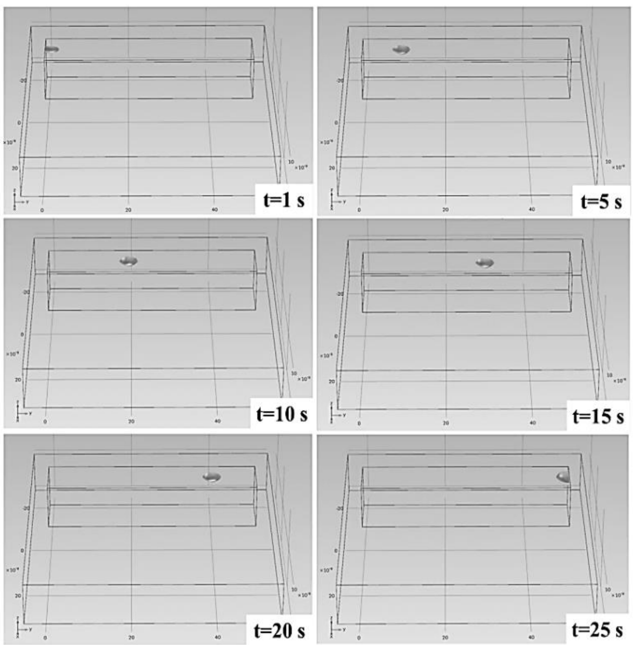

Fig. 8 Iso-surface temperature plot at 1605 K

The results of the developed model were compared with the real results measured and reported elsewhere [9]. The effect of the power and the scanning velocity on the depth (or height) of the deposition layer were studied.

Published By:
Blue Eyes Intelligence Engineering
and Sciences Publication (BEIESP)

It was assumed that the power source is 600W and the laser source diameter is 3 mm. As shown in Fig. 9, there is a good agreement between the simulated and the measured results that certifies the developed model. It is important to again mention that the value reported as the modeling result is the average value for all the seconds of the deposition. These values were extracted from the cross sections made at different steps of the scan. Two examples of these cross sections are shown in Fig. 10. Moreover, the average molten depth and width were calculated from the exported time-temperature-location data generated by COMSOL software. The maximum error between the measured and simulated results in the plot shown in Fig. 9 is ~15%.

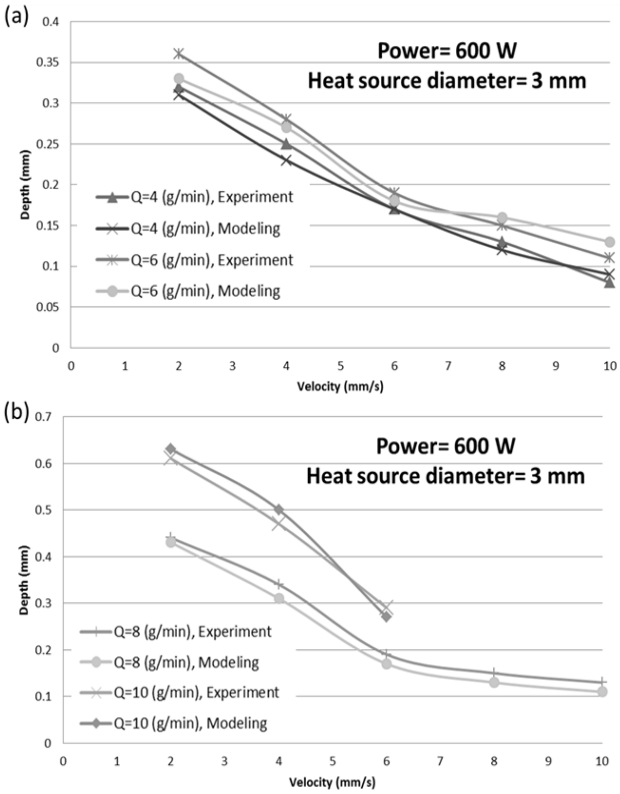

Fig. 9 Comparison of the experimental and computational results

Another validation of the thermal model was done based on considering the heat source velocity of 6 mm/s and the powder feeding rate of 4 g/min. The results of the experimental measurements as well as the modeling results are plotted in Fig. 11. The maximum error between the measured and simulated results in the plot shown in Fig. 11 is ~13%. Similar calculations were valid for the width comparison between the modeling and the experimental results. In accordance with Fig. 9 and Fig. 11, the comparison was made between the experimental results and the developed thermal model based on the width of the deposition. These results are shown in Fig. 12 and Fig. 13, respectively. The maximum errors between the measured and simulated results in the plots shown in Fig. 12 and Fig. 13 are ~14% and ~16%, respectively.

Generally speaking, there is no accurate way to control the amount of powder fed by the nozzle. Therefore, it is wise to feed more powder in each layer of the deposition. After the deposition process is done, it is easy to remove the powder by using air pressure. Regarding the amount of powder added to the system, in this paper, it is mentioned in terms of the weight percent per minute. The reason why they did not report the value based on the height is the fact that powders are perforate materials; i.e., there is an uncontrollable space between the powder particles. This space can change the exact height of the deposition. Therefore to avoid any shortage of powder during the deposition, extra powder is added in each layer of the deposition. At the end, the not-melted powder is removed from the deposited area by air pressure. Notably, the melting point of Nickel superalloy (1605 K) is far less than the melting point of the steel (~1833 K). Therefore, it is impossible to melt the steel while we still have some not-melted powder in our deposition system.

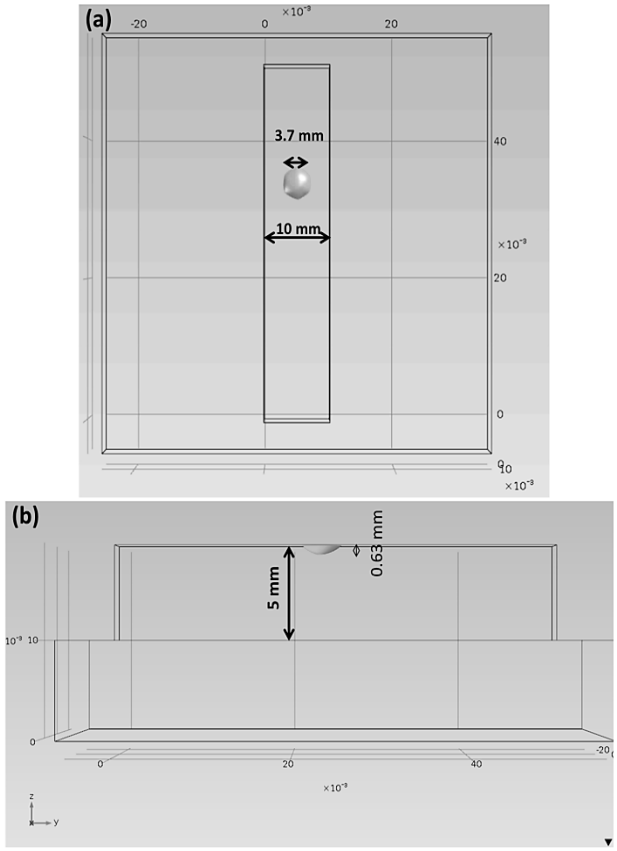

Fig. 10 Cross-section of the molten pool from *x-z* and *y-z* views

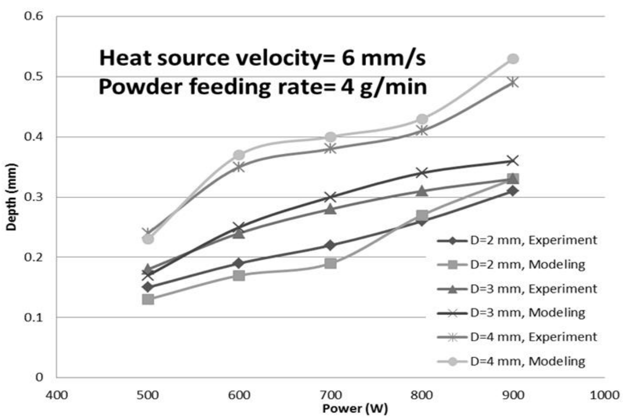

Fig. 11 Results comparison for the heat source velocity of 6 mm/s and the power feeding rate of 4 g/min

Published By:
Blue Eyes Intelligence Engineering
and Sciences Publication (BEIESP)

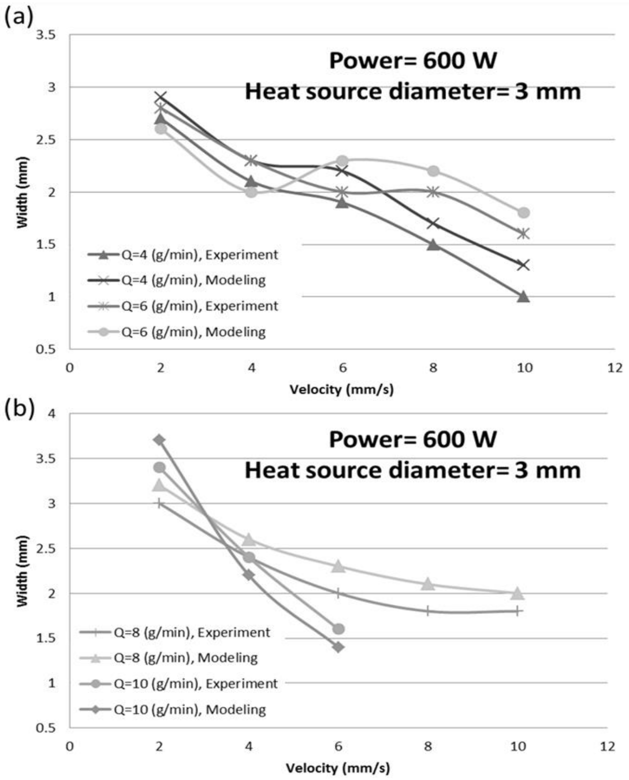

Fig. 12 Results comparison based on the width of the deposition

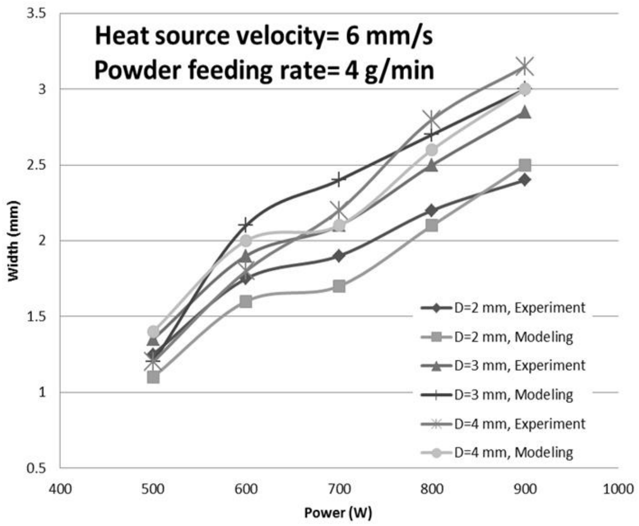

Fig. 13 Deposition width comparison for the heat source velocity of 6 mm/s and power feeding rate of 4 g/min

IV. CONCLUSIONS

In this study, a thermal model was developed based on the parameters mentioned in literature related to the deposition of nickel superalloy powder on steel substrate under argon atmosphere. There is a good agreement between the results predicted by the developed thermal model and the experimental results. There are some issues such as asymmetric molten pool with the thermal model that were discussed. This thermal model can be used to optimize the parameters involved in the deposition. For example, it is possible to change the speed of the scan based on the molten pool dimension or the rate of cooling required for achieving specific mechanical properties.

ACKNOWLEDGEMENT

The author acknowledges the department of mechanical and manufacturing engineering of Universiti of Putra Malaysia.

REFERENCES

[1] W. Hofmeister, M. Wert, J. Smugeresky, J. A. Philliber, M. Griffith, and M. Ensz, "Investigation of solidification in the laser engineered net shaping (LENSTM) process" *JOM*, Vol. 51, No. 7, 1999, pp. 1-6.

[2] A. Vasinonta, J. Beuth, and M. Griffith, "Process maps for laser deposition of thin-walled structures" In: *Proceesings of Solid Freeform Fabrication*, Austin, 1999, pp. 383-391.

[3] P. C. Collins, C. V. Haden, I. Ghamarian, B. J. Hayes, T. Ales, G. Penso, V. Dixit, and G. Harlow, "Progress toward an integration of process–structure–property–performance models for "three-dimensional (3-D) printing" of titanium alloys" *JOM*, Vol. 66, No. 7, 2014, pp. 1299-1309.

[4] J. Beuth, and N. Klingbeil, "The role of process variables in laser-based direct metal solid freeform fabrication" *JOM*, Vol. 53, No. 9, 2001, pp. 36-39.

[5] L. Costa, T. Reti, A. Deus, and R. Vilar, "Simulation of layer overlap tempering kinetics in steel parts deposited by laser cladding" In: *Proceedings of International Conference on Metal Powder Deposition for Rapid Manufacturing*, Princton, 2002, pp. 172-176.

[6] L. Wang, S. Felicelli, Y. Gooroochurn, P. Wang, and M. Horstemeyer, "Numerical simulation of the temperature distribution and solid-phase evolution in the LENS™ process" In: *Proceedings of the Seventeenth Solid Freeform Fabrication Symposium*, Austin, 2006, pp. 453-463.

[7] V. Neela, and A. De, "Three-dimensional heat transfer analysis of LENSTM process using finite element method" *The International Journal of Advanced Manufacturing Technology*, Vol. 45, No. 9-10, 2009, pp. 935-943.

[8] R. B. Patil, and V. Yadava, "Finite element analysis of temperature distribution in single metallic powder layer during metal laser sintering" *International Journal of Machine Tools and Manufacture*, Vol. 47, No. 7, 2007, pp. 1069-1080.

[9] K. Zhang, W. Liu, and X. Shang, "Research on the processing experiments of laser metal deposition shaping" *Optics & Laser Technology*, Vol. 39, No. 3, 2007, pp. 549-557.

A. Soleymani did his M.S. at the department of mechanical and manufacturing engineering at University of Putra Malaysia. He has widely worked on the modeling and simulations of various transport phenomena using finite element methods.

Published By:
Blue Eyes Intelligence Engineering and Sciences Publication (BEIESP)